ICENS 6TH INTERNATIONAL CONFERENCE ON ENGINEERING AND NATURAL SCIENCE
October 21-25 2020 Belgrade

Wireless Capsule Localization Inside the Human Small Intestine Using a Permanent Cube-Shaped Magnet with Analytical Magnetic Model

Muzaffer Kanaan[1], Memduh Suveren [2]

Abstract

Wireless Capsule Endoscopy (WCE) is a non-invasive technique used to visualize the digestive system in the human body. Many gastrointestinal (GI) system diseases such as Crohn's disease, tumor, bleeding, and polyps can be easily diagnosed with WCE. In recent years, the tendency to WCE method has been increasing especially in order to eliminate the disadvantages of traditional colonoscopy (being painful, risk of infection, completely dependent on operator skill, psychologically disturbing the patient). Here, together with the diagnosis made with the WCE technique, determining the location of the disease detected in the intestine is of great importance for the medical specialist. Therefore, this study focused on determining the position of WCE in the intestine. In this study, a cube-shaped magnet was used together with the wireless capsule, and the predicted positions of the wireless capsule in the small intestine were obtained using magnetic sensors placed on the human body model and the LM-ABC optimization algorithms. As a result, 5D (3D position, 2D orientation) localization procedure was performed with the analytical magnetic model of the cube magnet.

Keywords: Wireless Capsule Endoscopy, In-body Localization, LM algorithm, ABC algorithm

1. INTRODUCTION

Wireless capsule endoscopy is a painless and non-invasive diagnostic technique used in the digestive system, especially to view the small intestine [1]. WCE is especially used to visualize sections of the small intestine that are difficult to access with conventional endoscopy techniques. In this imaging method, a wireless capsule which has camera, battery, processor and wireless transmitter is swallowed [2]. The capsule moves passively with peristaltic contractions of the intestine in the GI tract, and the camera inside the capsule takes pictures and transmits the images to the outside via a wireless transmitter. These images taken are then analyzed by the specialist for the diagnosis and treatment of diseases. The aim of this technique, which is currently used today, is not only to diagnose but also to provide treatment. This is possible with active capsule endoscopy [3]. Active capsule endoscopy is basically manipulating the wireless capsule inside the body and changing capsule positions and angles from the outside by the specialist. The most important problem for active capsule endoscopy is that the position and orientation of the capsule should known precisely.

There are many studies on capsule localization in the literature. These are generally in the form of positioning with electromagnetic waves (radio frequency, visible waves, X-ray, Gamma ray), magnetic localization and other techniques (MRI, ultrasound) [4]. Although X-ray and Gamma ray techniques promise real-time and precise results, the biggest disadvantage of these techniques is that they have harmful effects on human health [5]. MRI and Ultrasound methods require extra space in the capsule and power consumption, so these techniques are not used much. In positioning with radio waves, high frequency signals are subjected to significant attenuation as they pass through body tissues [6]. Different tissue types (skin, muscle and bone) all have frequency-dependent propagation characteristics and adversely affect the transmission of RF signals [7]. For this reason, positioning errors are relatively higher in RF positioning in the body, since there is no direct line of sight between the sensor and the antenna [8]. On the other hand, magnetic localization method is being

[1] *Erciyes University, Department of Mechatronic Engineering, 38038, Melikgazi/Kayseri, Turkey.* mkanaan@erciyes.edu.tr

[2] *Corresponding author: Erciyes University, Department of Mechatronic Engineering, 38038, Melikgazi/Kayseri, Turkey.* msuveren@erciyes.edu.tr

studied because it does not require a direct line of sight and low-frequency static magnetic signals pass through body tissues without interaction as they pass through the air [9, 10].

Magnetic flux density generated by a permanent magnet or a current-controlled coil is used for magnetic localization. The position and angle of the magnet or coil can be calculated by means of previously known magnetic flux equations and hall effect sensors that measure these fluxes. Various magnetic flux equations are used in the literature such as Dipole model, finite difference method, Biot-Savart method and charge model. Then, optimization algorithms are used in solving the magnetic flux equations. In this study, the charge model equations of a cube-shaped permanent magnet were obtained and positioning studies were carried out using Artificial Bee Colony (ABC) and Levenberg-Marquardt (LM) optimization algorithms. The LM method, frequently used in positioning algorithms, is a combination of two minimization methods: the gradient descent method and the Gauss-Newton method [11]. ABC algorithm is an optimization algorithm based on a certain intelligent behavior of honeybee swarms in nature [12]. These two algorithms have been used together in this study to eliminate the disadvantages of each other and to make more precise positioning as in the previous study [13].

In this study, we gave information about the simulation environment in Section 2, obtained the analytical model for the magnetic localization algorithm in Section 3, and discussed the results in Section 4.

2. SIMULATION ENVIRONMENT

In simulations, it is aimed to obtain 5D (3D position and 2D angle) parameters of the magnetic capsule. It is assumed that a permanent cube-shaped magnet is placed at the back of the capsule to localize the capsule. Here, while the magnetic capsule moves inside the body, especially in the small intestine, the videos and images it sends to the external environment are matched with the location in the intestine. In order to see more realistic results, capsule locations were determined according to the real human intestine, not randomly. For this, 3-D voxel model data of the human body developed under the Visible Human Project [14] as shown Figure 1 was used.

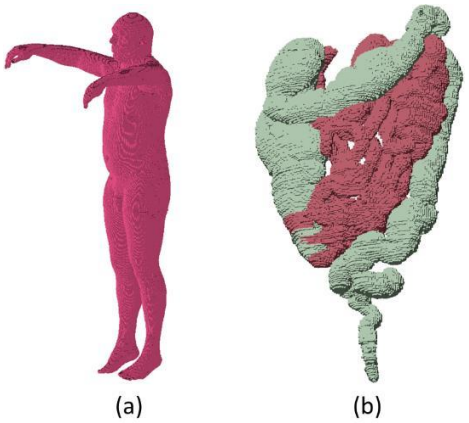

Figure 1. 3-D voxel models of the human body: a) The full body model, b) The intestine model

In the simulations, real magnet positions and angles were obtained for 80 different capsule locations in the small intestine. The magnet positions were homogeneously distributed in the area of 195x115x290mm. Here, the orientation of the capsule was determined to remain within the intestine. In addition, 9 sensors that measure magnetic flux, were placed on the body. Sensors were placed on the body at equal intervals and contacted the body. Thus, the actual sensor positions were taken over the body model, such as the capsule positions. These sensor and capsule locations are shown in Figure 2.

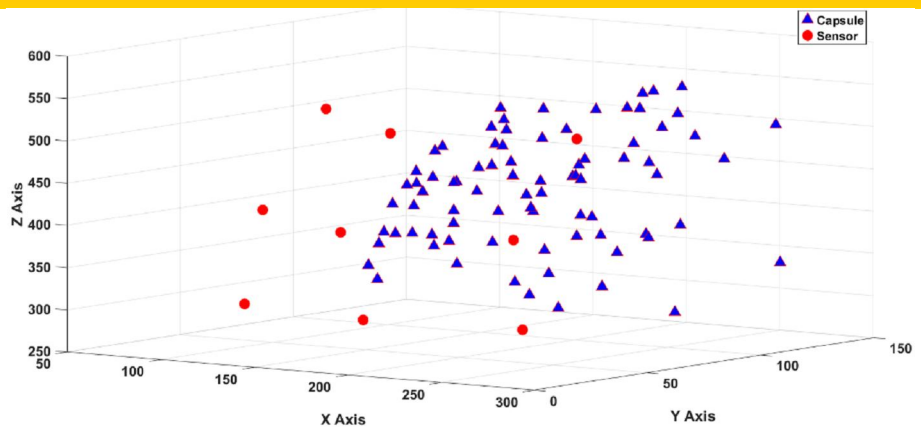

Figure 2. Sensor and Capsule positions in the body (mm)

The cube-shaped magnet structure shown in Figure 3 was used in the simulations. Each side length of the magnet is determined as 4mm. Thus, there will be no problem in capsule endoscopy since the magnet will not take up much space behind the capsule. The magnet also provides uniform magnetization in the z-axis direction and the **M** value is set as 830.000 (A/m) for the neodymium permanent magnet (NdFe35).

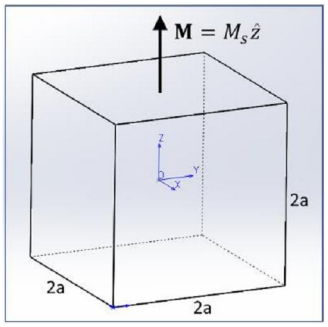

Figure 3. Cube Shaped Magnet

3. LOCALIZATION ALGORITHM

The localization algorithm consists of 3 parts: Analytical model, ABC optimization algorithm and LM algorithm. The working scheme of the localization algorithm is given in Figure 4.

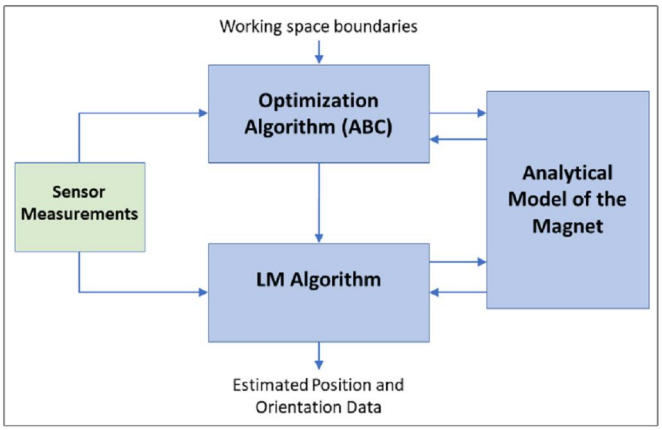

Figure 4. Working Scheme of the Localization Algorithm

The magnetic flux data calculated from the sensors on the body are given as an input to both the ABC algorithm and the LM algorithm. Here, the ABC algorithm generates the initial position parameters required for the LM algorithm. Both algorithms use the analytical magnetic model of the cube magnet to estimate the position and orientation parameters of the capsule.

3.1. Analytical Model of the Cube-Shaped Magnet

In magnetically positioned wireless capsule endoscopy, generally ring and quadrangular shaped magnets are used. While the magnetic fluxes of permanent magnets are obtained, the current model, charge model and finite difference method are mostly used in the literature. Here, magnetic flux equations of the magnet are created using the charge model. In this model, a magnet is reduced to a distribution of equivalent ‘‘magnetic charge’’. The charge distribution is used as a source term in the magnetostatic field equations, and the fields are obtained using standard methods [15]. The general magnetic flux equation given in Equation 1 is used to calculate the magnetic flux with the charge model.

$$\mathbf{B}(\mathbf{x}) = \frac{\mu_0}{4\pi}\int_V \frac{\rho_m(\mathbf{x}')(\mathbf{x}-\mathbf{x}')}{|\mathbf{x}-\mathbf{x}'|^3}dv' + \frac{\mu_0}{4\pi}\iint_S \frac{\sigma_m(\mathbf{x}')(\mathbf{x}-\mathbf{x}')}{|\mathbf{x}-\mathbf{x}'|^3}ds' \tag{1}$$

Here, the magnetic flux equation consists of two integrals containing volume (ρ_m) and surface (σ_m) charge density. Here, the volume charge density will be 0 in empty space, the surface charge density changes as in Equation 2 depending on the coordinates of the magnet given in Figure 3.

$$\rho_m = -\nabla\cdot\mathbf{M} = 0$$
$$\sigma_m = \mathbf{M}\cdot\hat{\mathbf{n}} = \begin{cases} M_s & (z=z_2) \\ -M_s & (z=z_1) \end{cases} \tag{2}$$

In Cartesian coordinates the integral form of the magnetic flux is found as in Equation 3 using Equations 1 and 2 [15].

$$\mathbf{B}(x,y,z) = \frac{\mu_0 M_s}{4\pi}\left(\int_{y_1}^{y_2}\int_{x_1}^{x_2}\frac{((x-x')\hat{\mathbf{x}}+(y-y')\hat{\mathbf{y}}+(z-z_2)\hat{\mathbf{z}})}{((x-x')^2+(y-y')^2+(z-z_2)^2)^{3/2}}dx'dy' - \int_{y_1}^{y_2}\int_{x_1}^{x_2}\frac{((x-x')\hat{\mathbf{x}}+(y-y')\hat{\mathbf{y}}+(z-z_1)\hat{\mathbf{z}})}{((x-x')^2+(y-y')^2+(z-z_1)^2)^{3/2}}dx'dy'\right) \tag{3}$$

At Equation 3; The expressions (*x, y, z*) represent the coordinates of the point where the flux value is calculated, and (x', y', z_1, z_2) represent the coordinates (boundaries) of the magnet. Since **B**(*x,y,z*) equation is vectorial, the x, y and z components are calculated separately.

$$\mathbf{B}_x(x,y,z) = \frac{\mu_0 M_s}{4\pi}\sum_{k=1}^{2}(-1)^k\int_{y_1}^{y_2}\int_{x_1}^{x_2}\frac{(x-x')dx'dy'}{((x-x')^2+(y-y')^2+(z-z_k)^2)^{3/2}}$$
$$= \frac{\mu_0 M_s}{4\pi}\sum_{k=1}^{2}\sum_{m=1}^{2}(-1)^{k+m}\int_{y_1}^{y_2}\frac{dy'}{((x-x_m)^2+(y-y')^2+(z-z_k)^2)^{1/2}} \tag{4}$$
$$= \frac{\mu_0 M_s}{4\pi}\sum_{k=1}^{2}\sum_{m=1}^{2}(-1)^{k+m}\ln\left(\frac{(y-y_1)+((x-x_m)^2+(y-y_1)^2+(z-z_k)^2)^{1/2}}{(y-y_2)+((x-x_m)^2+(y-y_2)^2+(z-z_k)^2)^{1/2}}\right)$$

$$\mathbf{B}_y(x,y,z) = \frac{\mu_0 M_s}{4\pi}\sum_{k=1}^{2}(-1)^k\int_{y_1}^{y_2}\int_{x_1}^{x_2}\frac{(y-y')dx'dy'}{((x-x')^2+(y-y')^2+(z-z_k)^2)^{3/2}}$$
$$= \frac{\mu_0 M_s}{4\pi}\sum_{k=1}^{2}\sum_{m=1}^{2}(-1)^{k+m}\int_{x_1}^{x_2}\frac{dx'}{((x-x')^2+(y-y_m)^2+(z-z_k)^2)^{1/2}} \tag{5}$$
$$= \frac{\mu_0 M_s}{4\pi}\sum_{k=1}^{2}\sum_{m=1}^{2}(-1)^{k+m}\ln\left(\frac{(x-x_1)+((x-x_1)^2+(y-y_m)^2+(z-z_k)^2)^{1/2}}{(x-x_2)+((x-x_2)^2+(y-y_m)^2+(z-z_k)^2)^{1/2}}\right)$$

$$\mathbf{B}_z(x,y,z)=\frac{\mu_0 M_s}{4\pi}\sum_{k=1}^{2}(-1)^k\int_{y_1}^{y_2}\int_{x_1}^{x_2}\frac{(z-z_k)dx'dy'}{((x-x')^2+(y-y')^2+(z-z_k)^2)^{3/2}}$$

$$=\frac{\mu_0 M_s}{4\pi}\sum_{k=1}^{2}(-1)^k\int_{y_1}^{y_2}\int_{x-x_1}^{x-x_2}\frac{(z-z_k)d\alpha dy'}{(\alpha^2+(y-y')^2+(z-z_k)^2)^{3/2}},\qquad \alpha=x-x'$$

$$=\frac{\mu_0 M_s}{4\pi}\sum_{k=1}^{2}\sum_{n=1}^{2}(-1)^{k+n+1}(z-z_k)(x-x_n)\int_{y_1}^{y_2}\frac{dy'}{\left[(y-y')^2+(z-z_k)^2\right]\left((y-y')^2+(x-x_n)^2+(z-z_k)^2\right)^{1/2}} \tag{6}$$

$$=\frac{\mu_0 M_s}{4\pi}\sum_{k=1}^{2}\sum_{n=1}^{2}\sum_{m=1}^{2}(-1)^{k+n+m}\arctan\left[\frac{(x-x_n)(y-y_m)}{(z-z_k)}\frac{1}{\left((x-x_n)^2+(y-y_m)^2+(z-z_k)\right)^{1/2}}\right]$$

$$\mathbf{B}(x,y,z)=B_x(x,y,z)\hat{\mathbf{x}}+B_y(x,y,z)\hat{\mathbf{y}}+B_z(x,y,z)\hat{\mathbf{z}} \tag{6b}$$

The magnet boundaries specified in Equations 4, 5 and 6 will be as follows, as shown in Figure 3.

$$(x_1,y_1,z_1)=-a,\ (x_2,y_2,z_2)=a$$

The magnetic flux equations obtained are defined according to the magnet's own local coordinate system. However, calculations need to be made in the global coordinate system in which the magnet and sensors are located together as shown in Figure 5. For this, when calculating the magnetic flux value of any point in space, this point must be reduced to the local coordinate of the magnet with transformation matrices.

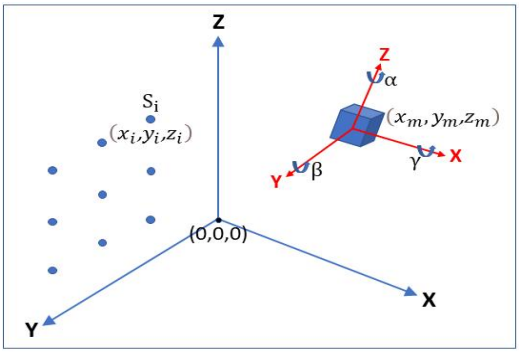

Figure 5. Global and Local Coordinate System of the Magnet

When Figure 5 is examined, Si represents the sensor on the body and (x_i, y_i, z_i) are the sensor location, (x_m, y_m, z_m) represents the magnet (capsule) position, and (γ, β, α) represents the magnet angles. The rotation matrix (**R**) calculated between the two coordinate systems is as in Equation 7.

$$\mathbf{R}=\begin{bmatrix}\cos(\alpha).\cos(\beta) & \cos(\alpha).\sin(\beta).\sin(\gamma)-\sin(\alpha).\cos(\gamma) & \cos(\alpha).\sin(\beta).\cos(\gamma)+\sin(\alpha).\sin(\gamma)\\ \sin(\alpha).\cos(\beta) & \sin(\alpha).\sin(\beta).\sin(\gamma)+\cos(\alpha).\cos(\gamma) & \sin(\alpha).\sin(\beta).\cos(\gamma)-\cos(\alpha).\sin(\gamma)\\ -\sin(\beta) & \cos(\beta).\sin(\gamma) & \cos(\beta).\cos(\gamma)\end{bmatrix} \tag{7}$$

In order to find the unknown positions and angles of the magnet ($x_m, y_m, z_m, \gamma, \beta, \alpha$), known sensor positions and magnetic flux values measured by sensors are used. As a result, the 6 unknown parameters of the magnet are calculated by Equation 8.

$$\begin{aligned}(B_{Xi},B_{Yi},B_{Zi})&=\mathbf{B}(x_{iL},y_{iL},z_{iL}).\mathbf{R}\\(x_{iL},y_{iL},z_{iL})&=\left[(x_i,y_i,z_i)-(x_m,y_m,z_m)\right].\mathbf{R}^{-1}\end{aligned} \tag{8}$$

where (x_{iL}, y_{iL}, z_{iL}) are the position of the ith sensor with respect to local coordinate system, **B** is the analytical magnetic flux vector at the Equation 6b and (B_{Xi}, B_{Yi}, B_{Zi}) are the measured magnetic flux value of the ith sensor. In the equation here, flux values and sensor coordinates measured by the sensors are known, and it is aimed to obtain magnet positions and angles. Since there are 6 unknowns in total, a minimum of 6 sensor data

is required. As a result, optimization algorithms are used to calculate magnet position and orientation parameters which are unknown in the equation. The optimization algorithm tries to predict the magnet positions and angles that will provide the magnetic flux values calculated by the sensors. For this, the cost function given in Equation 9 is used in the optimization algorithm.

$$\varepsilon = \sum_{i=1}^{N}\left[(B_{xi}-\hat{B}_{xi})^2+(B_{yi}-\hat{B}_{yi})^2+(B_{zi}-\hat{B}_{zi})^2\right] \tag{9}$$

where (B_{xi},B_{yi},B_{zi}) are the known calculated magnetic flux value of the ith sensor, $(\hat{B}_{xi},\hat{B}_{yi},\hat{B}_{zi})$ are the estimated magnetic flux value by optimization algorithm, N is the number of the sensor and ε is the error. The optimization algorithm aims to minimize this error value, ideally to make it 0.

3.2. LM Algorithm and ABC Optimization Algorithm

Artificial Bee Colony algorithm is an algorithm based on swarm intelligence such as Ant Colony Optimization, Particle Swarm Optimization, Artificial Fish Swarm Algorithm etc. The ABC algorithm is the adaptation of the intelligent behaviors of bees while finding nectar in nature to optimization algorithms [12]. Although the ABC algorithm provides satisfactory results when used alone, it is relatively slow in terms of computation time [16], like other swarm intelligence based algorithms. Therefore, the ABC algorithm is not used to find the exact magnet positions and angles, but to create an initial value for the LM algorithm.

Levenberg-Marquardt algorithm is the most widely used method in the literature to solve nonlinear least squares problems. LM algorithm basically uses Gradient-descent and Gauss-Newton methods in a single algorithm [11]. This enables the LM algorithm to provide both fast and precise solutions in the calculation of nonlinear equations. The disadvantage of the LM algorithm is that it requires precise initial values to produce solutions. If the initial values are unrealistic, the algorithm performance decreases significantly. For this reason, ABC and LM algorithms are used together in this study to complement each other.

Finally, performance analysis of the magnet position and angle values estimated by ABC-LM algorithms is made. For this purpose, the equations given in Equations 10 and 11 are used.

$$E_P = \sqrt{(x_m-\hat{x}_m)^2+(y_m-\hat{y}_m)^2+(z_m-\hat{z}_m)^2} \tag{10}$$

$$E_O = \cos^{-1}(\vec{V}_{real}(\gamma,\beta,\alpha)\cdot\vec{V}_{est}(\hat{\gamma},\hat{\beta},\hat{\alpha})) \tag{11}$$

where $(x_m,y_m,z_m,\gamma,\beta,\alpha)$ are the known real location parameters of the magnet, $(\hat{x}_m,\hat{y}_m,\hat{z}_m,\hat{\gamma},\hat{\beta},\hat{\alpha})$ are the estimated location parameters, E_P is the position estimation error and E_O is the orientation estimation error.

4. RESULTS

While estimating 5D position and angle of the wireless capsule, the simulation conditions given in Section 2 and localization algorithm given in Section 3 were used. ABC and LM algorithms were used together in all simulations and the parameters outside the population were kept constant. Since ABC and LM algorithms give different results in each iteration in the same run, the algorithms were run 10 times in each scenario and the averaged results were obtained. In simulations, wireless capsule localization process was performed for 5 different population numbers of ABC algorithm and the results obtained for 80 different points were averaged. These comparative results are given in Table 1.

Table 1. Comparison of capsule positioning performance depending on ABC population size

Population size of the ABC Algorithm	Mean Position Error (mm)	Max. Position Error (mm)	Mean Orientation Error (˚)	Max. Orientation Error (˚)	Time per Calculation (sn)
10	1,679	17,780	2,688	48,241	0,263
20	1,126	12,041	1,823	36,938	0,449
30	0,769	10,949	1,227	21,998	0,616
40	0,630	5,716	1,037	17,261	0,800
50	0,596	6,547	0,962	15,236	1,018

When the table is examined, it is seen that as the population number increases, position and angle errors decrease, and the calculation time increases. It is seen that the result is less than 1 second in all scenarios, also the average position error and the average angle error are below 1.7 mm and 2.7˚, respectively. The results of position error and angle error for 30 population size scenario are given in Figure 6 and Figure 7.

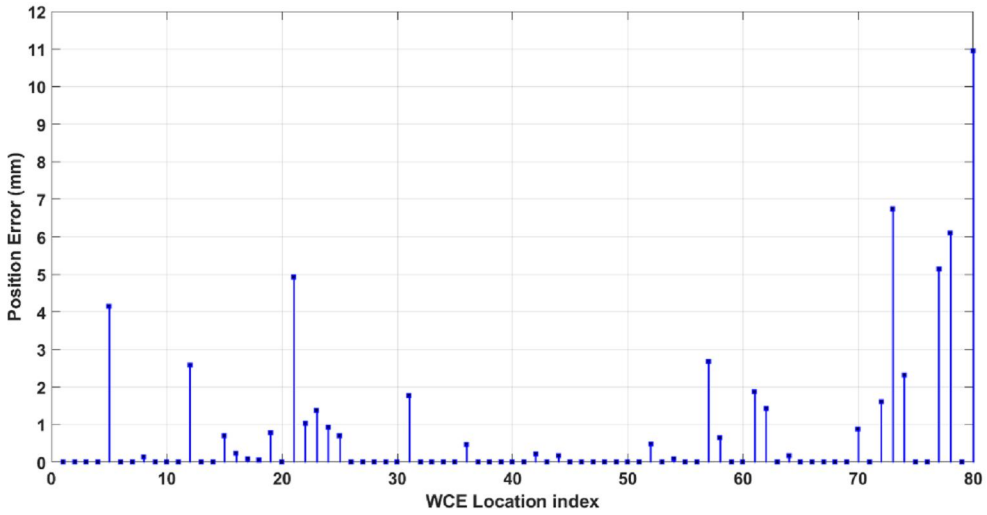

Figure 6. Position Error for ABC with 30 populations

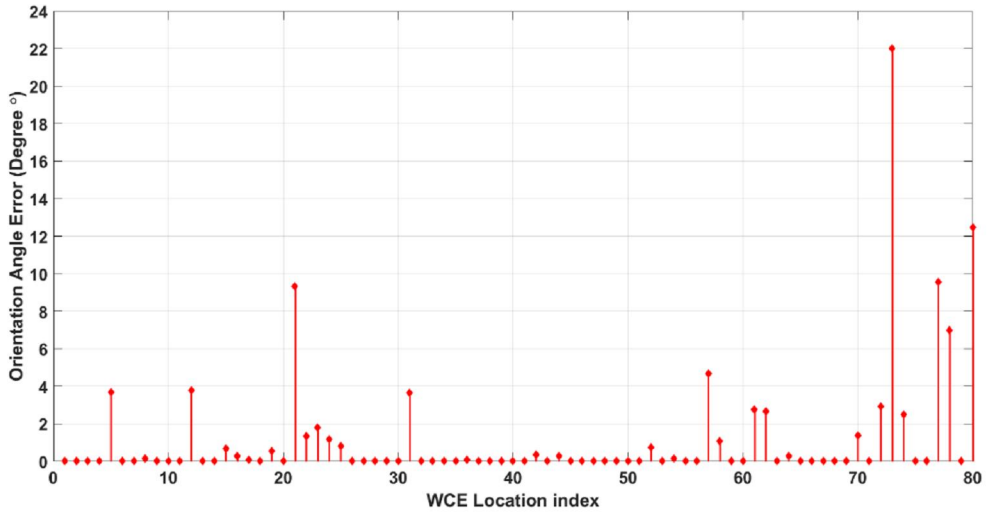

Figure 7. Orientation Error for ABC with 30 populations

When the figures obtained for 30 populations are examined, the position error of 71 out of 80 capsule locations (89%) is less than 2 mm. Similarly, the orientation angle error of 67 out of 80 capsule locations (84%) is less than 2˚. Also, analysis for each point was completed in about 0.6 seconds for 30 population scenario. These errors will come to much lower levels in offline working conditions and higher population values. However, in this study, a low number of populations were used in order to prepare for real-time simulations. These results pave the way for solving precise WCE localization problems in real time.

5. CONCLUSIONS

In this paper, we discussed the problem of localization of the wireless capsule in the small intestine using analytical model of the cube shaped magnet. In the estimation of capsule positions and angles, the results for different population scenarios were investigated by using both ABC and LM optimization algorithms. Our

results show that the mean position error value is below 1.68 mm and these results are obtained in a maximum of 1 second. Results can pave the way for more accurate localization in the wireless capsule endoscopy field.

ACKNOWLEDGMENT

This study was supported by the Erciyes University Scientific Research Projects Unit under grant number FDK-2018-7833.

REFERENCES

[1] P. Swain, G. J. Iddan, G. Meron, and A. Glukhovsky, "Wireless capsule endoscopy of the small bowel: development, testing, and first human trials," in *Biomonitoring and Endoscopy Technologies*, 2001, pp. 19-24.
[2] J. L. Toennies, G. Tortora, M. Simi, P. Valdastri, and R. J. Webster, "Swallowable medical devices for diagnosis and surgery: the state of the art," *Proceedings of the Institution of Mechanical Engineers, Part C: Journal of Mechanical Engineering Science,* vol. 224, pp. 1397-1414, 2010.
[3] G. Ciuti, A. Menciassi, and P. Dario, "Capsule endoscopy: from current achievements to open challenges," *IEEE reviews in biomedical engineering,* vol. 4, pp. 59-72, 2011.
[4] T. D. Than, G. Alici, H. Zhou, and W. Li, "A review of localization systems for robotic endoscopic capsules," *IEEE Transactions on Biomedical Engineering,* vol. 59, pp. 2387-2399, 2012.
[5] R. Kuth, J. Reinschke, and R. Rockelein, "Method for determining the position and orientation of an endoscopy capsule guided through an examination object by using a navigating magnetic field generated by means of a navigation device," ed: Google Patents, 2007.
[6] K. Yu, G. Fang, and E. Dutkiewicz, "Position and orientation accuracy analysis for wireless endoscope magnetic field based localization system design," in *2010 IEEE Wireless Communication and Networking Conference*, 2010, pp. 1-6.
[7] M. Kanaan and M. Suveren, "A novel frequency-dependent path loss model for ultra wideband implant body area networks," *Measurement,* vol. 68, pp. 117-127, 2015.
[8] M. Suveren, "Ultra Wide Band (UWB) Wireless Systems in Implant Body Area Networks and Modelling of the Distance Measurement Error," MSc Master Thesis, Mechatronic Engineering, Erciyes University, Kayseri, 2015.
[9] S. M. Aziz, M. Grcic, and T. Vaithianathan, "A real-time tracking system for an endoscopic capsule using multiple magnetic sensors," *Smart Sensors and Sensing Technology,* pp. 201-218, 2008.
[10] N. Atuegwu and R. Galloway, "Volumetric characterization of the Aurora magnetic tracker system for image-guided transorbital endoscopic procedures," *Physics in medicine and biology,* vol. 53, p. 4355, 2008.
[11] H. Gavin, "The Levenberg-Marquardt method for nonlinear least squares curve-fitting problems. 2011," *Availble Online from: http://people. duke. edu/~ hpgavin/ce281/lm. pdf..(Accessed 16 April 2019),* 2016.
[12] D. Karaboga and B. Basturk, "A powerful and efficient algorithm for numerical function optimization: artificial bee colony (ABC) algorithm," *Journal of global optimization,* vol. 39, pp. 459-471, 2007.
[13] M. Suveren and M. Kanaan, "On the Use of Human Body Models in Wireless Capsule Endoscopy Localization based on Ultra Wide Band Signaling," in *5th International Conference on Engineering and Natural Sciences (ICENS)*, Prague, 2019.
[14] M. J. Ackerman, " Viewpoint: The Visible Human Project, Journal Biocommunication, 18,2, p. 14.," 1991.
[15] E. P. Furlani, *Permanent magnet and electromechanical devices: materials, analysis, and applications*: Academic press, 2001.
[16] M. Suveren and M. Kanaan, "5D Magnetic Localization for Wireless Capsule Endoscopy Using the Levenberg-Marquardt Method and Artificial Bee Colony Algorithm," in *2019 IEEE 30th International Symposium on Personal, Indoor and Mobile Radio Communications (PIMRC Workshops)*, 2019, pp. 1-6.